JOURNAL OF THERMOPHYSICS AND HEAT TRANSFER
Vol. 6, No. 3, July–Sept. 1992

Experimental Verification of Scaling Parameters for Thermal Stratification

H-C. Ji*
Washington University, St. Louis, Missouri 63130
S. H. Schwartz†
California State University, Northridge, California 91330
T. N. Lovrich‡
McDonnell Douglas Corporation, Long Beach, California 90808
J. I. Hochstein§
Memphis State University, Memphis, Tennessee 38152
and
L. A. Holmes†
Modesto College, Modesto, California 95350

A study to determine important dimensionless parameters associated with thermal stratification of a heated container of liquid, and the pressure history of its vapor, was performed. Analysis of the governing equations identified the modified Grashoff number, the modified Fourier number, and the interface number as the dominant dimensionless parameters associated with this process. A test program designed to verify the validity of these scaling parameters was executed. The quality of scaling was checked by comparing the dimensionless pressures and temperatures for scaled pairs of tests. Results indicate that the bulk liquid temperature, the surface temperature of the liquid, and the tank pressure can be scaled with the three dimensionless parameters. Some deviations were found in the detailed temperature profiles between the scaled pairs of tests.

Nomenclature

C = specific heat
D = tank diameter
d = nozzle diameter
Fo^* = modified Fourier number, $\mu\theta/\rho D^2$
Gr^* = modified Grashoff number, $g\beta q'' L^4/k\nu^2$
g = gravitational constant
h_{fg} = latent heat of vaporization
I^* = interface number, $h_{fg}k_l/q''DC$
k = thermal conductivity
Ma^* = Marangoni number, $(q''D^2/k_l\mu_l\alpha_l)\partial\sigma/\partial T$
Pr = Prandtl number
p = pressure
q'' = heat flux
Re_j = jet Reynolds number
T = temperature
t = time
u = velocity in x direction
v = velocity in y direction
x = spatial coordinate
y = spatial coordinate
α = thermal diffusivity, $k/\rho C$
β = coefficient of thermal expansion
θ = stratification test period
μ = dynamic viscosity
ν = kinematic viscosity
ρ = density
σ = coefficient of surface tension
τ = dimensionless time, t/θ

Subscripts
j = jet
l = liquid
v = vapor

Received March 13, 1990; revision received Dec. 31, 1990; accepted for publication Jan. 8, 1991.

*Research Assistant, Department of Mechanical Engineering. Member AIAA.
†Professor, Department of Mechanical Engineering.
‡Lead Engineer, Space Division.
§Associate Professor, Department of Mechanical Engineering. Associate Fellow.

Introduction

MANY future space missions will rely on long-term storage of cryogenic propellants and will require appropriate storage and fuel transfer systems. The feasibility of these mission concepts and design configurations will be strongly influenced by the ability to design an efficient cryogenic propellant storage system. Consequently, it is important that the designer has a strong technical platform from which to predict required tank design pressures and thermodynamic and fluid dynamic behavior in a low-gravity environment.

Although considerable ground-test data have been gathered, and numerous analyses carried out in the area of propellant thermal stratification (and destratification), the basic scaling parameters that provide the relationship between the ground model tests and the full-scale flight vehicle performance have not been adequately substantiated. Prior studies have examined the basic physics of stratification, but they have not adequately examined the scaling of reduced-scale experimental results to actual propellant tank performance. Momenthy,[1] Bailey and Fearn,[2] and numerous other workers have used boundary-layer and lumped-mass analyses to predict stratification inside propellant tanks with mixed results. Tatom et al.,[3] using schlieren photographs, found that bottom heating and side heating of the tank produced noticeably different stratification patterns. Schwind and Vliet[4] observed that there is a complex interaction between the core flow and the boundary-layer flow at the walls and near the free surface. Aydelott[5,6] examined the effect of several parameters on the

self-pressurization of a liquid hydrogen propellant tank. He found that the rate of pressure rise was lower for reduced-gravity conditions than under normal-gravity conditions and that the location of the heat source was an important factor in determining the self-pressurization rate.

Chin et al.[7] conducted stratification experiments with three different size cylindrical tanks and correlated the data using a modified Grashoff number, Prandtl number, dimensionless time, and a dimensionless surface temperature. They found that the dimensionless temperature profile was time-invariant over the range of Grashoff numbers tested, and that the integrated energy determined over the range of modified Grashoff numbers was independent of the fluid used. Their results indicate that dimensionless parameters are capable of scaling thermal stratification in propellant tanks.

The phenomena associated with thermal stratification are sufficiently complicated so that useful scaling parameters cannot be established by analytical means alone. Therefore, a systematic analytical and experimental study of scaling parameters for thermal stratification was undertaken to establish the validity of the proposed scaling groups. The equations describing the behavior of the liquid and its vapor were nondimensionalized and the resulting dimensionless parameters, modified Grashoff number, modified Fourier number, and an interface number, were used to define a test matrix. The test parameters were held constant for scaled pairs of experiments to determine whether the two test conditions produced scaled results. Three geometrically similar test tanks were designed and fabricated. A destratification jet orifice was located at the bottom of each tank. These tanks were capable of heating the liquid and its vapor, either separately or together, at various liquid levels. Temperature was measured using thermocouples located in the liquid region, the vapor region, the tank walls, and the tank insulation. The pressure was monitored by a pressure gauge and a pressure transducer located at the head of the tank.

The test matrix consisted of 20 scaling tests and an additional 17 tests for determining data reproducibility. During the tests, three scaling groups, Fo^*, Gr^*, and I^*, were maintained at constant values. These tests covered a range of Gr^* from 10^{14} to 10^{16}, Fo^* from 10^{-6} to 10^{-4}, and I^* from 7.54×10^{-3} to 2.42×10^{-1}. Destratification tests were conducted at the termination of each stratification test by activating a pump which produced an axial mixing jet. The jet Reynolds number ranged from 20,000 to 45,100.

Scaling Analysis

To identify the nondimensional parameters associated with the stratification process, the transport equations and boundary conditions that describe the heated liquid–vapor system were recast in dimensionless form. The first step was to write the dimensional transport equations and the boundary conditions specific to the tank geometry and the liquid–vapor system. The transport equations and boundary conditions are listed below.

Conservation of Mass:

$$\frac{\partial u}{\partial x} + \frac{\partial v}{\partial y} = 0 \tag{1}$$

Momentum Equation:

$$\frac{Du}{Dt} = \frac{\partial u}{\partial t} + u\frac{\partial u}{\partial x} + v\frac{\partial u}{\partial y} = -\frac{1}{\rho}\frac{\partial p}{\partial x} + \nu\nabla^2 u \tag{2}$$

$$\frac{Dv}{Dt} = \frac{\partial v}{\partial t} + u\frac{\partial v}{\partial x} + v\frac{\partial v}{\partial y} = -\frac{1}{\rho}\frac{\partial p}{\partial y} + \nu\nabla^2 v + g\beta\Delta T \tag{3}$$

Conservation of Thermal Energy:

$$\frac{DT}{Dt} = \frac{\partial T}{\partial t} + u\frac{\partial T}{\partial x} + v\frac{\partial T}{\partial y} = \frac{k}{\rho C}\nabla^2 T \tag{4}$$

The boundary conditions for the transport equations at a flat liquid–vapor interface are the equations for continuity of velocity and shear stress

$$u_l = u_v, \qquad \rho_l\nu_l\frac{\partial u_l}{\partial y} - \rho_v\nu_v\frac{\partial u_v}{\partial y} = \frac{d\sigma}{dT}\frac{dT}{dx} \tag{5}$$

continuity of temperature and heat flux at the liquid–vapor interface

$$T_v = T_l, \qquad k_l\frac{\partial T_l}{\partial y} - k_v\frac{\partial T_v}{\partial y} = \rho_l h_{fg}\frac{dy}{dt} \tag{6}$$

and the equations for specifying velocity and temperature at the tank walls

$$u_w = v_w = 0, \qquad q_l \text{ and } q_v - \text{Specified} \tag{7}$$

The next step in the process is to select characteristic scales to nondimensionalize independent and dependent variables. The characteristic values selected are: D = characteristic length (ft); $\rho_l D^3$ = characteristic mass (lbm); θ = characteristic time–stratification time (s); $q''_l D/k_l$ = characteristic temperature (°R); and $q''\theta/D$ = characteristic pressure (p_v) (lb_f/ft^2). The use of tank diameter as a characteristic length, and the liquid density as a characteristic mass is a commonly accepted practice in modeling. Here θ, or stratification test time, was defined to be the characteristic time, rather than $\sqrt{D/g}$. The wall heat flux q'' multiplied by the ratio D/k_l was used to define a characteristic temperature, because it is easily computed before vehicle flights or experiments. The heat input q'' is also used to characterize pressure. The characteristic pressure is derived by writing the perfect gas law

$$p_v = \rho_v R T_v \tag{8}$$

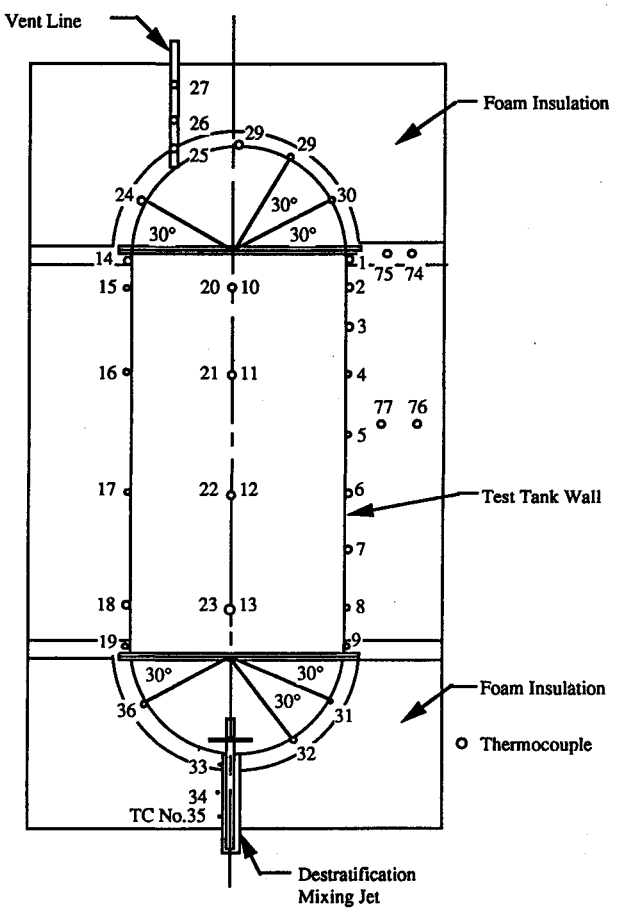

Fig. 1 Propellant test tank.

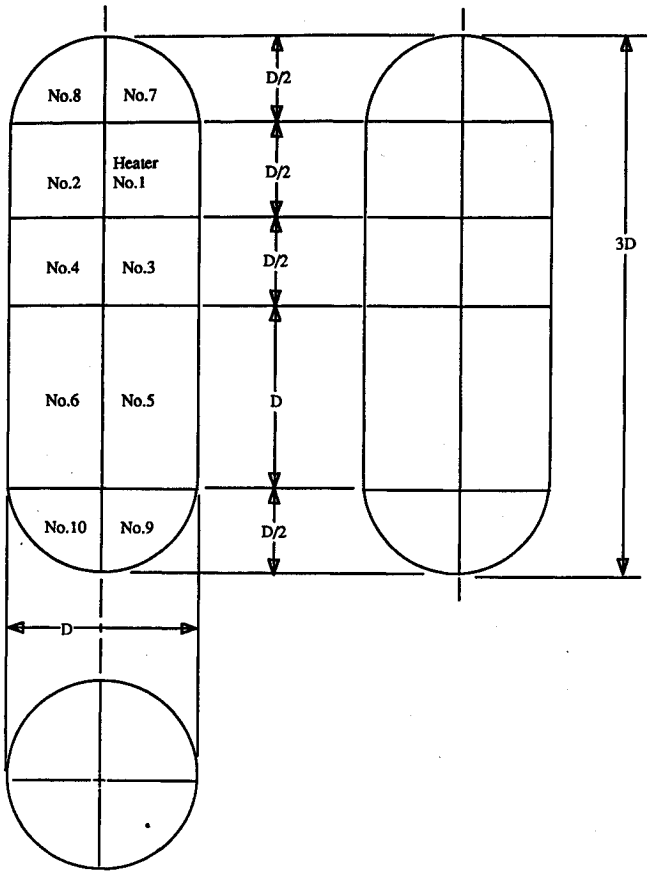

Fig. 2 Wall heater arrangement.

and nondimensionalizing the right-hand side with the characteristic temperature to yield

$$p_v = \left(\frac{q''\theta}{D}\right)\left(\frac{Pr}{Fo^*}\frac{R}{C_p}\right)\rho_v^* T_v^* \tag{9}$$

which indicates that the dimensional form $(q''\theta/D)$ may be used as a characteristic pressure, and the dimensionless pressure is given by

$$P_v^* = \frac{p_v}{(q''\theta/D)} \tag{10}$$

The characteristic scales are listed below:

$$x^* = \frac{x}{D} \qquad y^* = \frac{y}{D}$$

$$u^* = \frac{u}{D/q} \qquad v^* = \frac{v}{D/q}$$

$$p_v^* = \frac{p_v}{q''\theta/D} \qquad T^* = \frac{T}{q''D/k_l}$$

$$t = \frac{t}{\theta}$$

Using the selected characteristic scales to nondimensionalize the governing equations and associated boundary conditions produced the following results for the liquid phase.
Dimensionless Continuity:

$$\frac{\partial u^*}{\partial x^*} + \frac{\partial v^*}{\partial y^*} = 0 \tag{11}$$

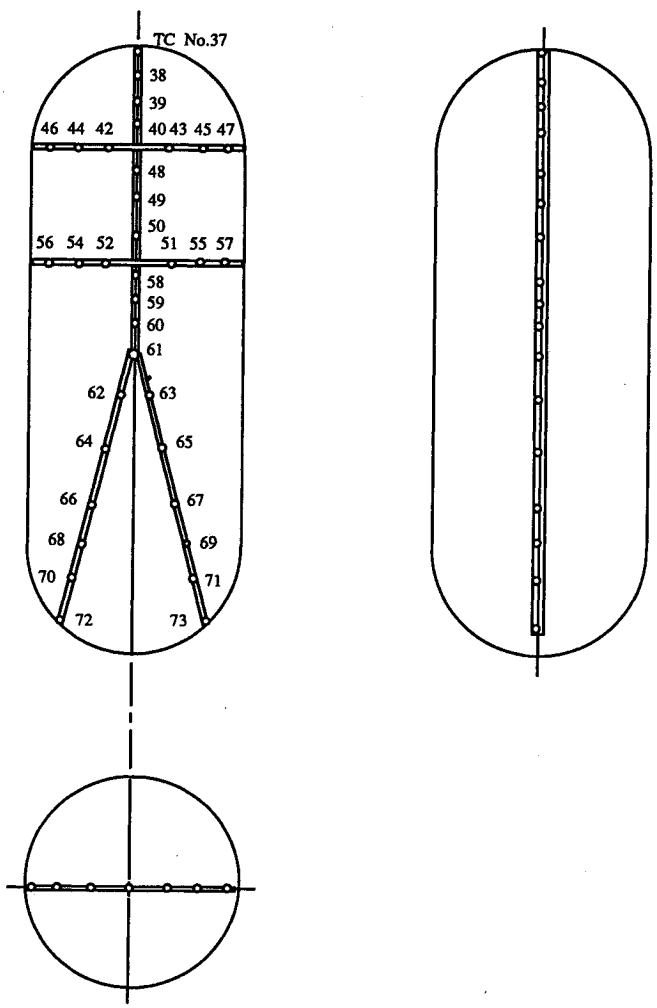

Fig. 3 Thermocouple rake arrangement.

Dimensionless Momentum:

$$\frac{Du^*}{Dt} = -\frac{1}{\rho}\frac{\partial p^*}{\partial x^*} + \frac{1}{Re}\nabla^2 u^* \tag{12}$$

$$\frac{Dv^*}{Dt} = -\frac{1}{\rho}\frac{\partial p^*}{\partial y^*} + \frac{1}{Re}\nabla^2 v^* + Fo^{*2}\cdot Gr^*\Delta T^* \tag{13}$$

Dimensionless Energy:

$$\frac{DT^*}{Dt} = \frac{Fo^*}{Pr}\nabla^2 T^* \tag{14}$$

Dimensionless Liquid-Vapor Interface Boundary Conditions:

$$k_l\frac{\partial T_l^*}{\partial y^*} - k_v\frac{\partial T_v^*}{\partial y^*} = \frac{\rho_l D h_{fg}}{q''\theta}\frac{dy^*}{d\tau}$$

$$= \frac{Pr}{Fo^*}\frac{h_{fg}k_l}{q''DC}\frac{dy^*}{d\tau} = \frac{Pr\cdot I^*}{Fo^*}\frac{dy^*}{d\tau} \tag{15}$$

$$\frac{\partial u_l^*}{\partial y^*} - \rho_v\frac{\nu_v}{\nu_l}\frac{\partial u_v^*}{\partial y^*} = \frac{q''\theta}{\rho_l\nu_l k_l}\frac{d\sigma}{dT}\frac{dT^*}{dx^*} = \frac{Fo^*}{Pr}\cdot Ma^*\frac{dT^*}{dx^*} \tag{16}$$

The five coefficients appearing in the nondimensional differential equations are the dimensionless scaling parameters:

$$Re_j = \frac{v_j d_j}{\nu_l} \text{ (jet mixing)} \tag{17}$$

$$Gr^* = \frac{g\beta_l q'' D^4}{\nu_l^2 k_l} \quad (18)$$

$$Fo^* = \frac{\mu\theta}{\rho D^2} \quad (19)$$

$$Ma^* = \frac{q'' D^2}{\mu_l k_l \alpha_l} \frac{d\sigma}{dT} \quad (20)$$

$$I^* = \frac{h_{fg} k_l}{q'' DC} \quad (21)$$

Since it is impossible to achieve complete similitude in a scale model test, it was necessary to identify which dimensionless groups are least significant so that emphasis could be directed toward the remaining groups. The Marangoni number is associated with motion at the liquid–vapor interface driven by a gradient in the coefficient of surface tension due to its temperature dependence. Because little variation of the temperature along the interface was expected, and no such motions were observed during flow visualization experiments conducted with Freon 113, the Marangoni number was not scaled. The basic scaling ideas are contained in Ref. 8.

Experimental Hardware and Procedure

The experimental system consisted of: three test tanks with identical (L/D) ratios capable of supplying heat through the walls, a centrifuge facility for high-gravity tests, and instrumentation required to regulate and monitor the tests. Freon-113 PCA (Precision Cleaning Agent) was chosen as the test fluid due to its relatively high boiling point (117°F), and because it is safe to handle with proper ventilation.

The three tanks are geometrically similar to the Modular Nuclear Vehicle and the Saturn S-IV-203 tanks. The test tanks are right circular cylinders with hemispherical dome caps at each end. The ratio of tank length to diameter is 3 for all tanks. The diameters are 6, 8, and 18 in. and the lengths are 18, 24, and 54 in., respectively. Thermocouples are placed as shown in Fig. 1 and the external surfaces of the tanks are wrapped with segmented heaters, as shown in Fig. 2. The heaters are capable of producing a maximum of 10 W/in.^{2} (4910 Btu/h-ft^2), and are encapsulated in foam insulation with a low thermal conductivity (0.01 Btu/h-ft-°F). Fluid temperature was monitored using a thermocouple rake (Fig. 3) located inside the tank which was designed to minimize interference with the fluid flow. The vapor pressure is monitored by a pressure transducer located at the top of the tank. A horizontal arm centrifuge is used to produce gravity levels of 8 g and 27 g for the 6-in. and 8-in. diam tanks, respectively. The high gravity levels are required to maintain the modified Grashoff number at constant values for the different tanks.

The thermal stratification test is initiated by heating the fluid using the wall heaters, thoroughly mixing the fluid with the jet, and waiting until the fluid temperature settled to the saturation temperature at 1 atm. The tank was not vacuum purged but was purged of air by repeated venting and replenishment of the tank contents. The tank top is then closed and the heaters are turned on. The heating is controlled so that heat can be selectively supplied to the fluid, to the vapor, or simultaneously to both regions. During stratification, the temperature is sensed at the 77 thermocouple locations and the vapor pressure is sensed by pressure gauge mounted at the head of the tank.

The test matrix for stratification, presented in Table 1, was developed to examine the validity of the dimensionless parameters identified by the scaling analysis. Scaled pairs of experiments were selected for various combinations of the three different sized tanks. These pairs were arranged to give the widest possible range of dimensionless number values.

Table 1 Stratification test matrix

Test column 1: 6-in.-diam tank		Test column 2:	Test column 3:
8 g	27 g	12-in.-diam tank, 1 g	18-in.-diam tank, 1 g
1000 Btu/h-ft^2 (L) 87.5% fill $Gr^* = 10^{15}$ tests #2, #12S		500 Btu/h-ft^2 (L) 87.5% fill $Gr^* = 10^{13}$ test #30, #25	
1000 Btu/h-ft^2 ($L+U$) 87.5% fill $Gr^* = 10^{15}$ tests #3, #11S		500 Btu/h-ft^2 ($L+U$) 87.5% fill $Gr^* = 10^{15}$ test #31, #17	
700 Btu/h-ft^2 ($L+U$) 50% fill $Gr^* = 10^{14}$ tests #9S, #15S		350 Btu/h-ft^2 (L) 50% fill $Gr^* = 10^{14}$ tests #33, #32	
700 Btu/h-ft^2 ($L+U$) 50% fill $Gr^* = 10^{14}$ tests #10S, #16S		350 Btu/h-ft^2 (L + U) 50% fill $Gr^* = 10^{14}$ tests #34, #35	
600 Btu/h-ft^2 ($L+U$) 87.5% fill $Gr^* = 7\times10^{14}$ tests #1, #5, #8S		300 Btu/h-ft^2 (L + U) 87.5% fill $Gr^* = 7\times10^{14}$ tests #20, #22	
600 Btu/h-ft^2 ($L+U$) 87.5% fill $Gr^* = 7\times10^{14}$ tests #4, #6		300 Btu/h-ft^2 (L + U) 87.5% fill $Gr^* = 7\times10^{14}$ tests #23, #28	
90 Btu/h-ft^2 ($L+U$) 87.5% fill $Gr^* = 10^{14}$ test #14		45 Btu/h-ft^2 (L) 87.5% fill $Gr^* = 10^{14}$ tests #26, #15	
90 Btu/h-ft^2 ($L+U$) 87.5% fill $Gr^* = 10^{14}$ test #13		45 Btu/h-ft^2 (L + U) 87.5% fill $Gr^* = 10^{14}$ test #27	
	2230 Btu/h-ft^2 (L) 50% fill $Gr^* = 10^{15}$ test #1S		748 Btu/h-ft^2 (L) 50% fill $Gr^* = 10^{15}$ tests #B, #D
	2880 Btu/h-ft^2 (L) 87.5% fill $Gr^* = 10^{16}$ test #3S		960 Btu/h-ft^2 (L) 87.5% fill $Gr^* = 10^{16}$ tests #IS

Notes: (L), liquid heating; ($L+U$), liquid + ullage heating. Tests horizontally across table are scaling tests (i.e., tests having constant modified Grashoff number $Gr^* = Gr_H^* = f(L$ = liquid depth); "S" in tests indicates no heating during destratification testing.

Table 2 Destratification test matrix

Test column 1: 6-in.-diam tank		Test column 2: 12-in.-diam tank, 1 g	Test column 3: 18-in.-diam tank, 1 g
8 g	27 g		
Tests #2, #12S Re_j = 38K, 38K		Tests #30, #25 Re_j = 38K, 31K	
Tests #3, #11S Re_j = 38K, 38K		Tests #31, #17 Re_j = 38K, 31K	
Tests #9S, #15S Re_j = 38K, 38K		Tests #33, #32 Re_j = 31K, 24K	
Tests #10S, #16S Re_j = 38K, 45.1K		Tests #34, #35 Re_j = 31K, 20K	
Tests #1, #8S, #5 Re_j = 31K, 38K, 31K		Tests #20, #22 Re_j = 31K, 31K	
Tests #4, #6 Re_j = 31K, 31K		Tests #23, #28 Re_j = 31K, 31K	
Test #14 Re_j = 38K		Tests #26, #15 Re_j = 31K, 25K	
Test #13 Re_j = 38K		Test #27 Re_j = 31K	
	Test #1S Re_j = 38K		Tests #BS, #D Re_j = 38K, 38K
	Test #3S Re_j = 45.1K		Test #IS Re_j = 45.1K

Notes: Re_j, Reynolds number of destratification (mixing) flow at nozzle exit; "S" indicates no destratification heating was applied.

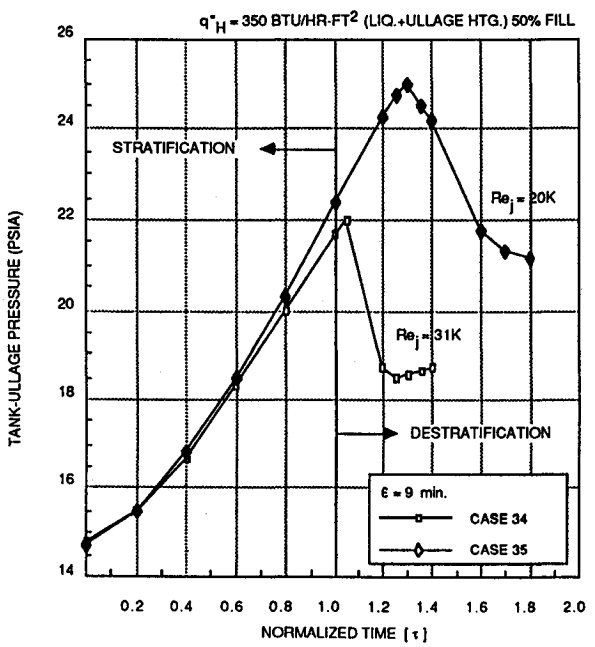

Fig. 4 Tank pressure history.

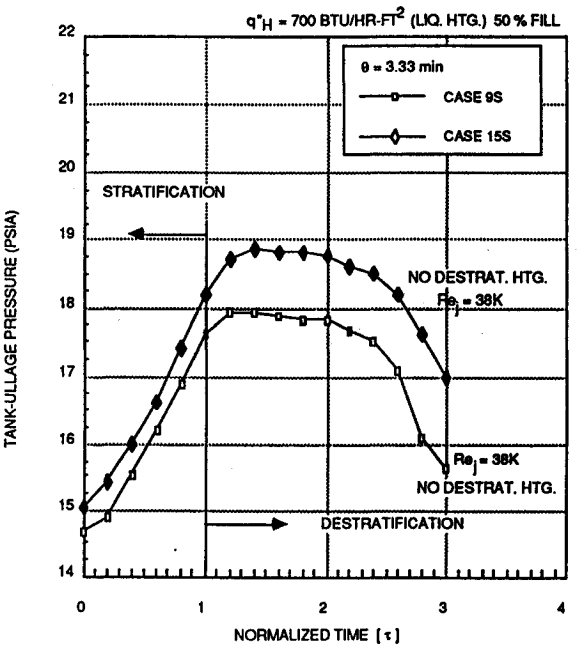

Fig. 5 Tank pressure history.

The three scaling parameters, (Gr^*, Fo^*, and I^*), were held fixed for the scaled pairs of tests. The tests were conducted using the 6-in.-diameter tank and either the 12-in. or 18-in.-diam tank. All tests were conducted with liquid heating and some with simultaneous ullage and liquid heating. The test matrix consisted of 20 scaling tests and 17 tests to examine data reproducibility. The tests covered a range of Gr^* from 10^{14} to 10^{16}, a range of Fo^* from 10^{-6} to 10^{-4}, and a range of I^* from 7.54×10^{-3} to 2.42×10^{-1}.

The range of the modified Grashoff numbers was limited by the allowable heating rates. For heat fluxes greater than 1000 Btu/h-ft^2, nucleate boiling is expected at atmospheric pressure. As pressure rises during a test, nucleate boiling becomes less likely. To avoid nucleate boiling at the walls and to protect the heater blankets, the maximum Grashoff number for tests in the test matrix was limited to 10^{16}. Rough estimates of the heat leak rate with the 12-in. tank were made from preliminary data which indicated that the value was

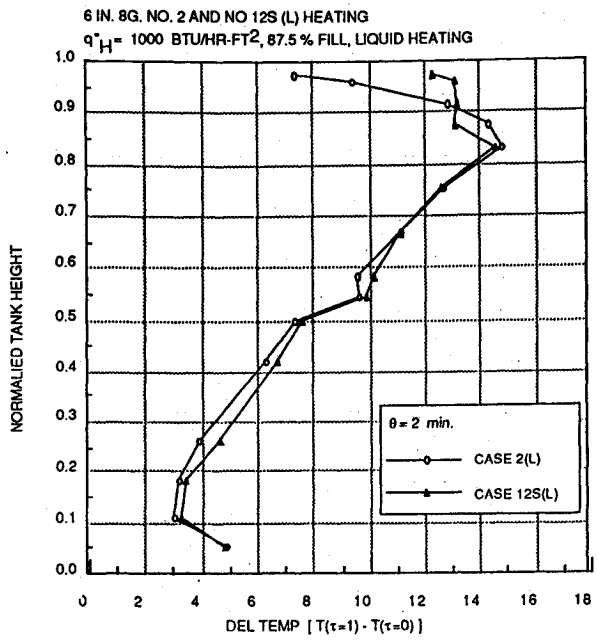

Fig. 6 Temperature reproducibility data.

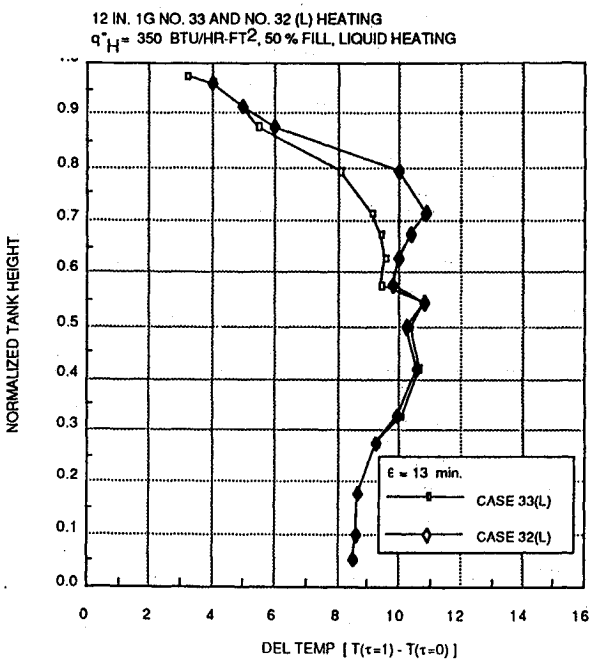

Fig. 7 Temperature reproducibility data.

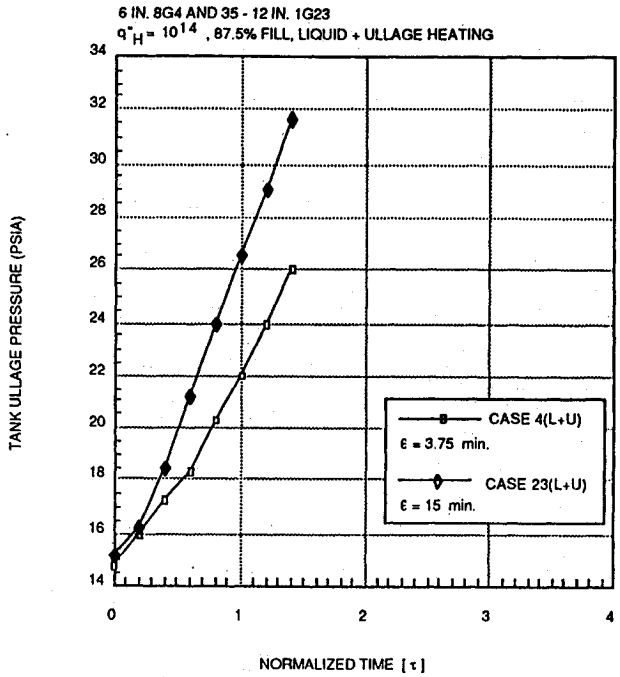

Fig. 8 Scaling pressure history.

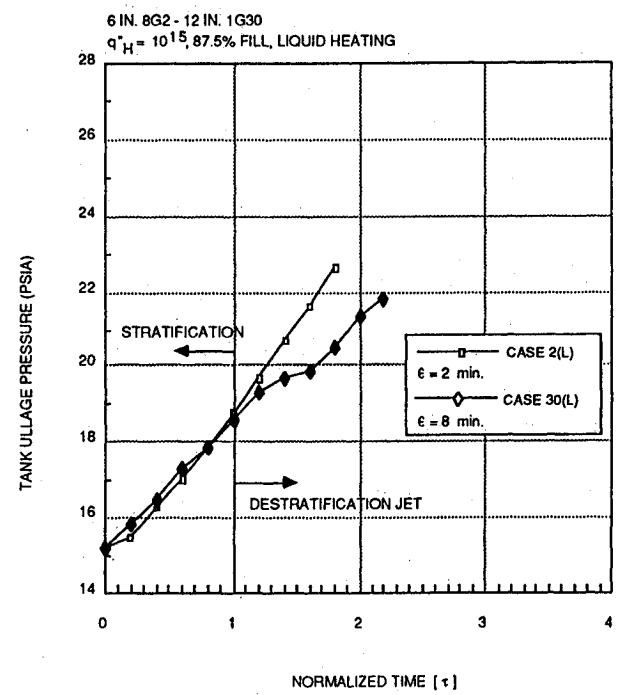

Fig. 9 Scaling pressure history.

between 1 and 10 Btu/h-ft^2. Therefore, 45 Btu/h-ft^2 was selected as the lower limit for heat flux. This condition corresponds to a modified Grashoff number of 10^{14}.

The stratification test period was defined as the elapsed time required to obtain a temperature rise of 15°F at the liquid free surface which corresponds to a pressure rise in the tank of 5 psig. A smaller rise could introduce significant error because the temperature increase should be at least an order of magnitude greater than the thermocouple resolution. A larger value approaches the safety limits of the tanks. Matching values for the interface number did not introduce any additional variables associated with the tank and thus did not impose further limits on the range of the experimental conditions. Tests were conducted with fluid fill levels of 87.5% and 50%.

The destratification experiments were performed at the conclusion of stratification tests. Destratification was accomplished by withdrawing fluid from the bottom of the tank and reinjecting it into the liquid pool through a nozzle with a diameter of 0.0104 tank diameters. The mixer operated until the temperature sensors and the ullage pressure sensor indicated that mixing had been achieved, or until it became apparent that the jet mixer could not overcome the prevailing convective currents. Some destratification tests were performed with the stratification heaters turned on, while others were performed with the heaters off. The vapor pressure was recorded during destratification, but the temperatures were not recorded. The test matrix for destratification is shown in Table 2.

Data Reproducibility

Data reproducibility was evaluated by comparing the pressure history and the temperature history for repeated tests with identical test conditions. Pressure data reproducibility

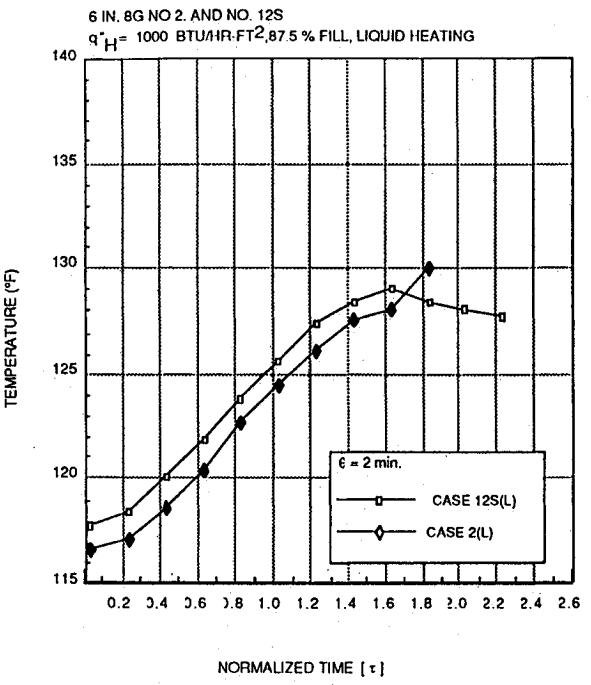

Fig. 10 Bulk liquid temperature history.

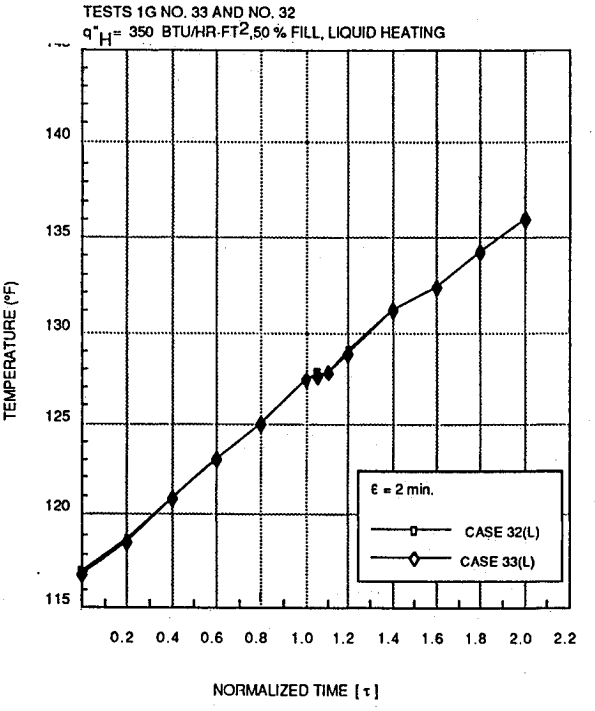

Fig. 11 Bulk liquid temperature history.

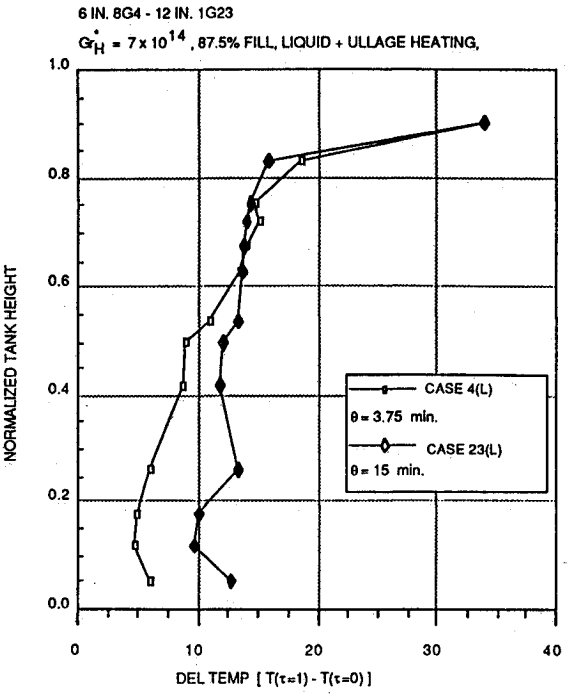

Fig. 12 Scaling temperature profiles.

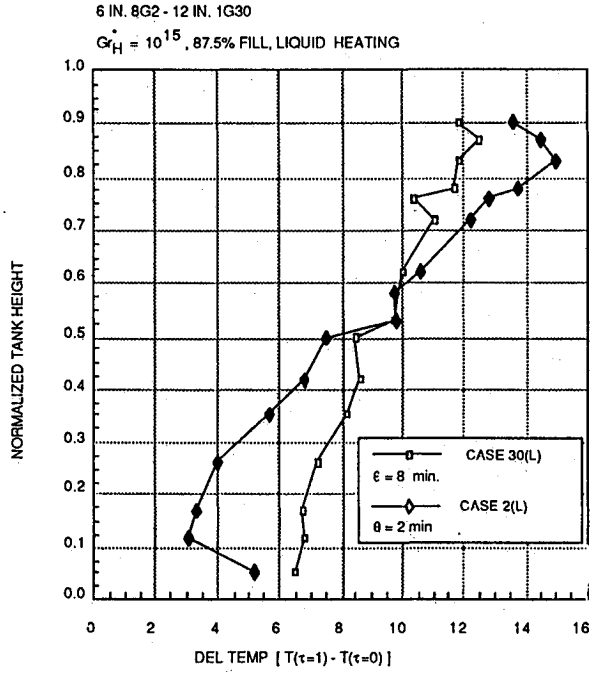

Fig. 13 Scaling temperature profiles.

was evaluated by comparing tank pressure percent deviations from identical sets of tests. The difference in pressure increase between the respective tests, divided by the averaged initial pressure, was used as a quantitative measure of pressure deviation. The calculated maximum relative deviation was less than 10% for all test cases. A tank pressure history for a pressure reproducibility test is shown in Fig. 4. Figure 5 depicts a test condition where the starting conditions were not identical, in part due to differences in barometric pressure; however, the pressure histories are parallel to each other.

Examination of the temperature profiles for identical test conditions revealed the scatter in the temperature values to be less than 2°F at each thermocouple location. Figures 6 and 7 show the temperature distributions at the end of a stratification test ($\tau = 1.0$). Based on the 17 reproducibility tests, the reproducibility of the experimental data was judged to be good.

Scaled Pair Results

Twenty pairs of tests were performed to evaluate the adequacy of the identified scaling parameters. A sampling of scaling test results is presented in Figs. 8–13. The full set of test results is presented in Ref. 9. Comparisons of pressure history data for dynamically similar conditions show that there is good agreement for liquid-only heating cases, shown in Figs. 8 and 9. The agreement is not as good for the combined liquid and vapor heating cases. The dimensionless tank pressure with liquid heating was scaled within 5.1% for the liquid only heating cases, and is 16–28% for the combined heating cases.

The quality of temperature scaling was determined by examining the bulk liquid temperature–time curves and the

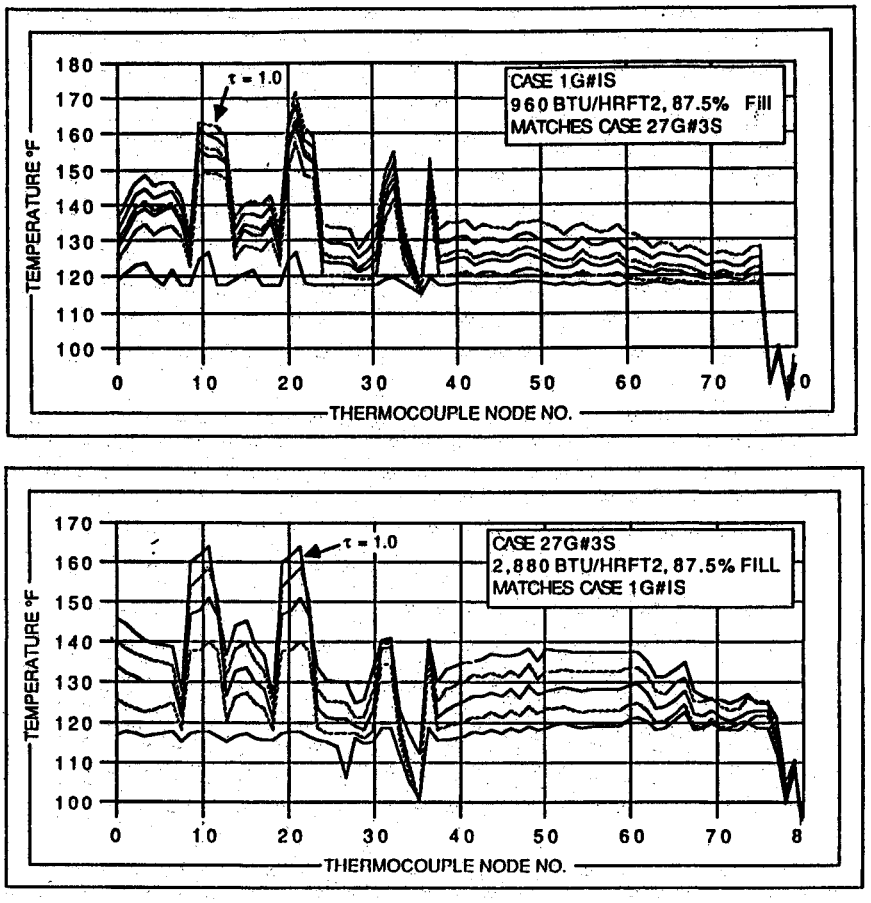

Fig. 14 Temperature profile for a 1-*g* to 27-*g* scaling test.

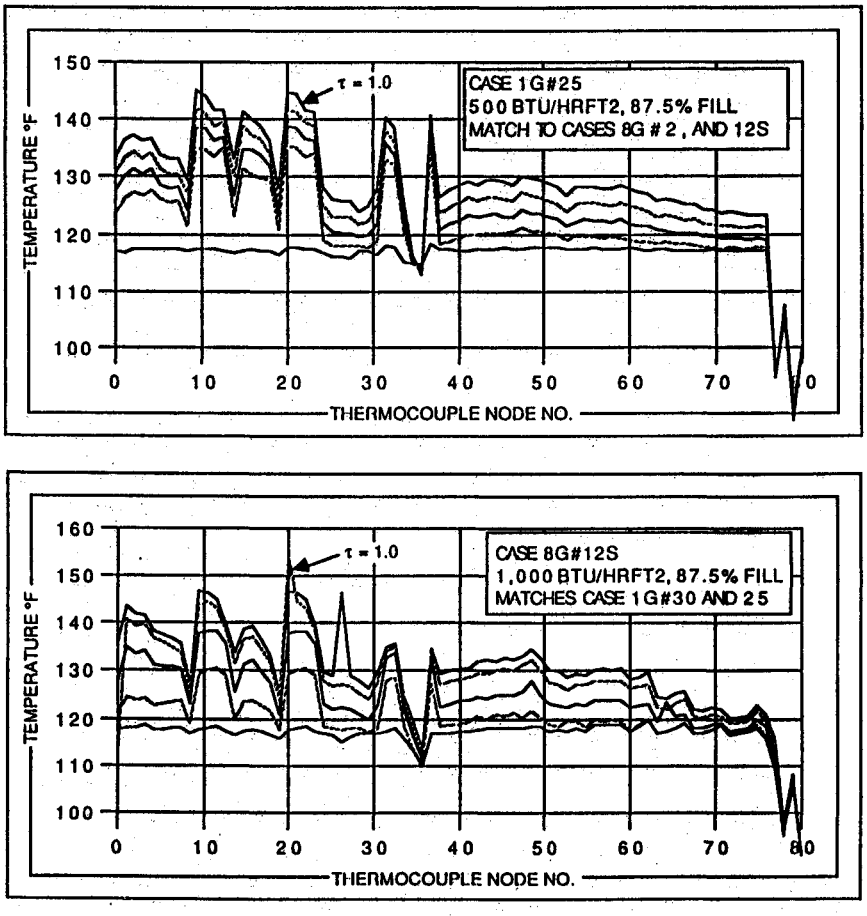

Fig. 15 Temperature profile for a 1-*g* to 8-*g* scaling test.

temperature profiles for $\tau = 1$. The bulk liquid temperature histories for the stratification tests scaled within 2.5%, and some cases are shown in Figs. 10 and 11. The bulk liquid temperature reflects the integrated temperature effect of the heat absorbed by the liquid. The experimental data show that the total energy transferred to the liquid was scaled reasonably well. Hence, overall heat transfer to the propellant tanks was well scaled, and the dimensionless parameters enable overall scaling of heat transfer to the propellant tank.

Free surface temperature deviations were about the same as the pressure deviations for the liquid heating cases. There are, however, noticeable differences, 10–39%, in the normalized temperature profiles for the scaled tests shown in Figs. 12 and 13. Because of the high degree of repeatability of the liquid-bulk temperature, as well as the point-by-point temperature match for identical sets of tests, it is likely that these differences are due to real thermodynamic and fluid dynamic differences in the separate tanks. One possible explanation is that constant thickness insulation was used for all three propellant tanks. Since in some instances it was found that the wall temperature for smaller tanks was higher than for larger tanks, and in other instances it was lower, the effect of insulation thickness on the temperature profiles is unclear. To ensure thorough scaling, future experiments should scale the insulation thickness.

As shown in Figs. 14 and 15, the temperature distribution measured by thermocouple nodes 40–70 during the 8-g and 27-g tests was consistently more jagged than that measured during the 1-g tests. Unlike the 1-g tests, the gravity vector for the high-gravity tests is not aligned with the tank axis so the buoyancy-induced flows are not symmetric with respect to the tank. This asymmetry may account for the rapid variation in temperature profiles at the higher gravity levels. Further, it may explain the inability of the scaling parameters to produce a good point-to-point match for the detailed temperature distributions.

Summary

The test program designed to verify the validity of scaling parameters for the propellant stratification process was successfully completed. An analysis of the governing equations yielded four dimensionless groups as candidates for scaling parameters: Gr^*, Fo^*, I^*, and Ma^*. The test program was designed around three geometrically similar tanks in which scaled pairs of tests with identical values for the Gr^*, Fo^*, and I^* were performed. Reproducibility tests demonstrated the adequacy of the experimental design and procedures. The identified scaling parameters were inadequate for producing a point-to-point temperature match between scaled pairs of tests.

The dimensionless scaling parameters were very successful in matching the bulk liquid mean temperatures, liquid-free surface temperature, and the vapor pressure history of the scaled pairs of tests. Although the curved liquid–vapor interface present in a zero-gravity environment may have an effect on the details of the stratification process, the fundamental scaling relationships verified by this study will still be valid. Furthermore, many projected applications, such as Orbit Transfer Vehicle propellant tanks, operate in a low-gravity rather than a zero-gravity environment. The combination of large tank diameter with a low-gravity environment can result in Bond numbers greater than 10, indicating that for these applications the interface is well approximated by the interface in the experimental tanks.

Based on the results of this study, we conclude that Gr^*, Fo^*, and I^* are the correct scaling parameters to relate the results of ground-based reduced-scale thermal stratification tests to the performance of propellant storage tanks in full-scale spacecraft.

Acknowledgment

This work was supported by George C. Marshall Space Flight Center through Contract NAS8-24747.

References

[1]Momenthy, A. M., "Propellant Tank Pressurization-System Analysis," *Advances in Cryogenic Engineering*, Vol. 9, 1963, p. 273.

[2]Bailey, T. E., and Fearn, R. F., "Analytical and Experimental Determination of Liquid-Hydrogen Temperature Stratification," *Advances in Cryogenic Engineering*, Vol. 9, 1963, p. 254.

[3]Tatom, J. W., Brown, W. H., Knight, L. H., and Coxe, E. F., "Analysis of Thermal Stratification of Liquid Hydrogen in Rocket Propellant Tanks," *Advances in Cryogenic Engineering*, Vol. 9, 1964, p. 265.

[4]Schwind, R. G., and Vliet, G. C., "Observations and Interpretations of Natural Convection and Stratification in Vessels," *Proceedings of the 1964 Heat Transfer and Fluid Mechanics Institute*, 1964, pp. 51–68.

[5]Aydelott, J. C., "Effect of Pressurization on Self-Pressurization of Spherical Liquid-Hydrogen Tankage," NASA TN D-4286, 1967.

[6]Aydelott, J. C., "Normal Gravity Self-Pressurization of 9 inch-(23 Cm) Diameter Spherical Liquid Hydrogen Tankage," NASA TN D-4171, 1967.

[7]Chin, J. H., Donaldson, J. O., Gallagher, L. W., Harper, E. Y., Hurd, S. E., and Satterlee, H. M., "Analytical and Experimental Study of Liquid Orientation and Stratification in Standard and Reduced Gravity Fields," Lockheed Missiles and Space Co., Rept. 1-05-64-1, July 1964.

[8]Lovrich, T. N., and Schwartz, S. H., "Development of Thermal Stratification and Destratification Scaling Concepts—Volume I. Stratification Experimental Data," NASA CR-143945, 1975.

[9]Lovrich, T. N., and Schwartz, S. H., "Development of Thermal Stratification and Destratification Scaling Concepts—Volume II. Stratification Experimental Data," NASA CR-143945, 1975.